A THERMO MECHANICAL ANALYSIS DURING CUTTING 2024-T351 ALUMINIUM ALLOY UNDER ABAQUS EXPLICIT

Farida Benabid[1], Mohamed Arrouf [2]

[1,2] "Mostepha Ben Boulaid" University of Batna2, Department of Mechanical Technology
University of Batna2, Avenue Chahid Boukhlouf 05001, Batna Algeria

Corresponding author: Farida Benabid, fari_b2003@yahoo.fr

Abstract: In this paper, heat transfer analysis during cutting 2024-T351 aluminium alloy with carbur tungsten (25° rake angle) and especially in 2, 3D orthogonal cutting operation numerically was performed. The assembly was modelled, meshed and analysed using commercial computational tool ABAQUS EXPLICIT. The parameters to be varied are depth of cut and impact speed, the thermal boundary conditions are adiabatic, the thermal contact between tool and workpiece is imperfect and the following method is Lagrangian, the results were well visualized and compared with literature, [23] and are in good agreement with reality of cutting.
It was found that maximum temperature turn around 400°C when cutting and it is located in chip formation on the other hand, heat conduction with impact speed were two antagonist phenomenon, in other terms, increase in impact speed has less effect on heat transfer and in conduction espescialy.

***Key words*:** Abaqus, moving heat sources, heat transfer, orthogonal metal cutting process, cuting temperature, adiabatic behavior.

1. INTRODUCTION

Many problems in cutting metal are related to the adequate cooling of tools and machine tools, this, in turn, requires knowledge of the mechanism by which heat is released from the cutting zone and transferred to the surrounding. Heat is transferred from one body to another in three differents ways, by conduction, convection and radiation, in the case of cutiing metal, there is a phenomenon denoted the adiabatic behavior which means that during cutting metal, there is no exchange of heat in the metal until at cutting zone where heat transfer is very important. Cutting temperature has to be predicted and controlled to prevent crater wear formation enhanced due to high temperatures in the rake face and thereby to prolong their life: the higher the temperature, the shorter their life and to keep temperature of the workpiece at a level drawn by the manufacturing.
The cutting temperature has severe effect on both tool and the workpiece life expectancy and in the inaccuracy dimensions. The cutting temperature has to be predicted and controlled, in order to optimize the cutting conditions and selecting tools geometries. The ductile material studied is the 2024-T351 aluminium alloy which is widely attracted in the manufacture of aerospace industry for its higher corrosion resistance, the melting point is one of the chief factors that determine the choise of metals, and in this case, it is not very high so it has to be controlled.
Heat is generated at cutting zone by a heavy plastic strain and friction at three zones:

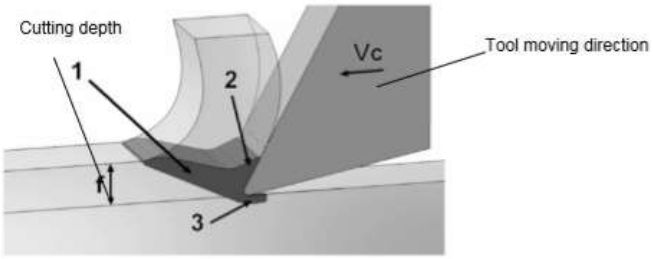

Fig. 1. The three plastic zones in metal cutting, [1]

✓90% of energy is converted into heat at the primary shear zone.
✓At the chip–tool interface, heat is generated due to rubbing and chip deformation.
✓At the worn out flanks due to rubbing between the tool and the finished surfaces, [2-4].
Loewen and Shaw have shown apportionment of heat which is carried by tool, chip and workpiece. The faster the cutting speed the greater the heat carried with the chip.
Cutting temperature can be determined by three ways, [17]:
✓Analytically using mathematical models for thermal field which can be developed. This method is simple, quick, inexpensive but less accurate, [5-7].
✓Experimentally, this method is always used because it is more accurate, precise and reliable, [8].
✓Numerically, this technique is widely used tools for thermal machining simulation and benefits the reduction of the cost and increase technical

performance, [9].
Three methods are utilized in the FEM these last decades: Lagrangian, Eulerian and ALE method, [10, 12]; the last method has been used mainly by several researchers in metal cutting for its performance in predicting field resuls, example: chip morphology, variables distribution. Tuğrul Özel and Erol Zeren, [13], utilize the advantages offered by ALE method in simulating plastic flow around the round edge of the cutting tool and eliminate the need for chip separation criteria. Ceretti et al. developed a cutting model by deleting elements having reached a critical value of accumulated damage.
During cutting simulation, flow stress, strain, strain rate (10^3 s^{-1}, 10^5 s^{-1}) and temperature are dependent at high degree because of complication phenomenon in the cutting zone, [23]; therefore analysis requires a coupled thermal stress equations in order to reach accurate predictions in FEM simulations**.**
In our work, we have analysed thermaly the behavior during cutting 2024-T351 aluminium alloy.
In view of the above literatures, the authors have found that there are less studies in the combined effect of impact velocity, depth of cut, temperature distribution during cutting metal, hence the study is done numerically under abaqus explicit by finite element, [20] in order to increase the accuracy in predicted results, a validation has been performed with literature and the predicting results holds good for both heat transfer and the reality of dynamic cutting.

2. MODEL PREPARATION

The tool is modeled to be as a rigid body perfectly [10,15], the workpiece is deformable $(0.002x0.005)m^2$.
In the case of high speed manufacturing, HSM, inelastic heat is required for simulations, here deformation will rise temperature due to the generated heating so properties of materials are function of temperature, in the heat balance equation, the generated heat is considered as heat source, generally, it is set to 0.9, this value is a fraction (Hong and Shaojian, 2013). Johnson&Cook, [16], constitutive model is widely used among models for workpiece plastic behavior description; it is a particular type of isotropic hardening, [15].

2.1. Tool and workpiece modelling

The tool and workpiece geometry is given by the figure below, figure 2.

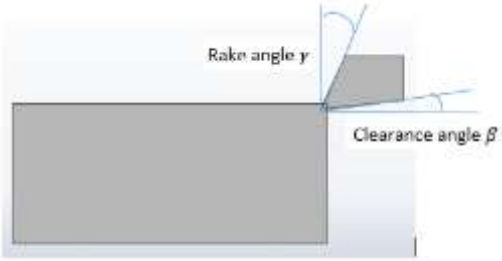

Fig. 2. The 2-D tool workpiece assembly

Table 1. Tool geometry variables

Rake angle γ [°]	Clearance angle β [°]
25	6

In thermal stresses analysis, we have to introduce mechanical and thermal properties of material, elasticity, plasticity and conductivity and so forth, also the coefficient of thermal expansion is included which will rise the material strain, table 2.

Table 2. Thermo physical properties of tool and workpiece

	Tungsten carbide	2024-T351 al. alloy
Young modulus (GPa)	800	72
Poisson ratio (-)	0.2	0.33
Coefficient of Thermal expansion (K^{-1})	0.0047 at 20°C 0.0049 at 1000 °C	0.011 at 20 °C
Thermal conductivity (W/mK)	46	200
Specific heat (J/kgK)	203	903
Density (K/m^3)	15000	2700

2.2. Plasticity Johnson & Cook constitutive model

Constitutive model of Johnson&Cook is widely used among models for workpiece plastic behavior description, [16], it is an isotropic hardening type, the initial yield stress, σ0 is given by equation (1):

$$\sigma^0 = [A+B\,(\acute{\varepsilon}^{pl})^{n}]\,[1+C.\ln\acute{\varepsilon}/\acute{\varepsilon}_0]\,[1-\Theta] \qquad (1)$$

Table 3. Johnson & Cook parameters, [23]

$\acute{\varepsilon}^{pl}$	The equivalent plastic strain (mm)	
A	initial yield stress [MPa]	352
B	hardening modulus [MPa]	440
C	strain rate dependency coefficient[-]	0.0083
n	work-hardening exponent [-]	0.42
m	thermal softening exponent [-]	1
Θ	Dimensioneless temperature [-]	
T_m	Melting temperature [K]	750
$\acute{\varepsilon}$	Strain rate (s^{-1})	1000
$\acute{\varepsilon}_0$	Strain rate reference	1

A, B, C, n and m are parameters of ductile material which are measured at or below the transition, T_{rans}.
In equation 1, the first term is the effect (strain hardening) of plastic strain, the second term represents the effect (viscous behavior) of strain rate, finally, the third term represents (thermal softening) the effect of temperature rise.

2.3. Johnson & Cook failure model

Failure accumulation in the Johnson-Cook model, [16], does not directly degrade the yield surface. The model of the strain at fracture is given by, [22]:

$$\varepsilon_{failure} = [C1+C2.\exp(C3\sigma^*)](1+C4.\ln\dot{\varepsilon}^*)(1+C5.\Theta^*) \quad (2)$$

where σ* is the ratio of the pressure to the effective stress, it is the stress triaxiality parameter, C1 to C5 are material failure canstants.

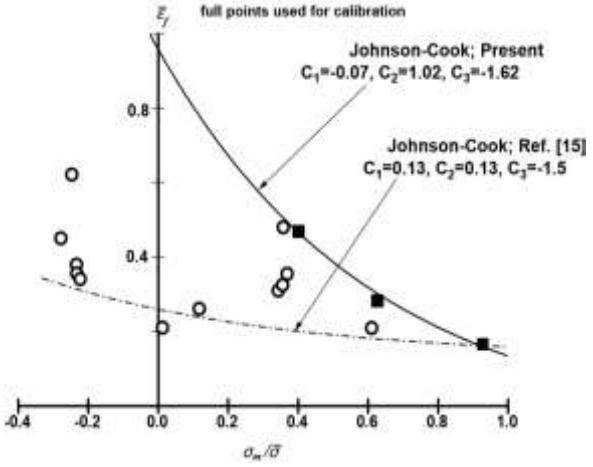

Fig. 3. Johnson & Cook failure canstants, [22]

Table 4. Johnson & Cook failure parameters

C1	C2	C3	C4	C5
0.13	0.13	-1.5	0.011	0

2.4. Heat generation at the interface tool/workpiece zone

The mechanical energy converted into heat is set to 100% and heat fraction which goes to workpiece is to be 0.5. At cutting zone, the contact is not perfect due to the important pression gradient between the stiking and the sliding region, hence a thermal contact resistance is introduced between aluminium and tungsten without intersticiel fluid and a high contact pression, $R_{ont}=2.10^{-6}$ K/W. A very drop in temperature occurs at contact zone.

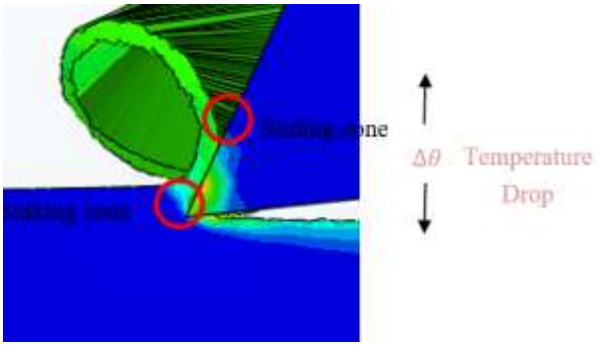

Fig. 4. Contact resistance in cutting zone

2.5. Mechanical conditions

Mechanical conditions are well visualized in the figure 5, the tool is alloyed to move along the horizontal direction of x, Vc varie from 10 mm/s to 200 mm/s, the workpiece is fixed.

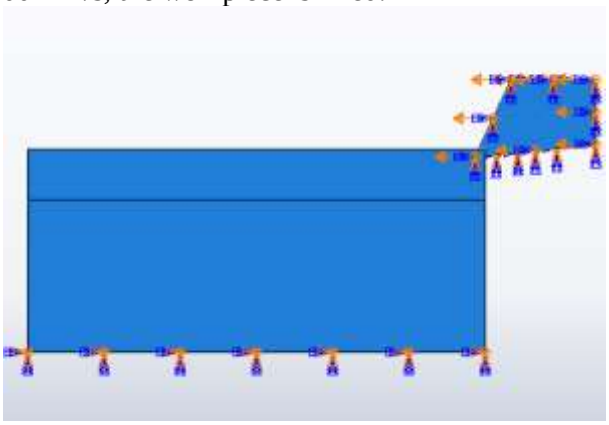

Fig. 5. Mechanical boundary conditions

2.6. Thermal conditions

The initial temperature is set to 25°C. One case of boundary conditions imposed is taken into account:
We assume an adiabatic condition: all faces of the tool/workpiece are adiabatic, such that all internal plastic work is converted into temperature change, there are no heat exchange between the wool with surroundings, however, in the contact, across the interface tool/workpiece, as it is seen, and there is contact conduction so heat going to workpiece is its thermal effusivity.

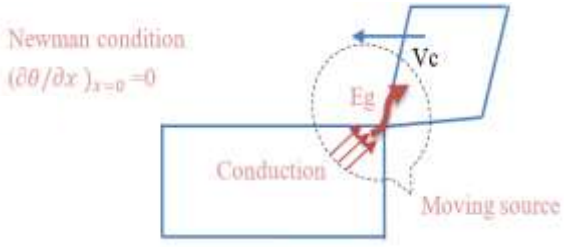

Fig. 6. Thermal boundary conditions

The governed equation (Ayed, 2017) of the adiabatic behavior is:

$$\Delta T=\beta\,[\sigma\Delta\varepsilon^p/\rho C_v] \quad (3)$$

where: σ is the effective stress and ε^p is the effective plastic strain, ρ is the mass density and C_v is the volumic specific heat and ΔT is the temperature change, β is the Taylor Quinney coefficient which represent the fraction of deformation energy transformed into heat.

3. RESULTS AND DISCUSSION

As shown in figure 7 and table 5, for low impact speed, the chip formation is circular and heat transfer is important, however for higher impact speeds, chip formation is quit linear and heat transfer is very low.

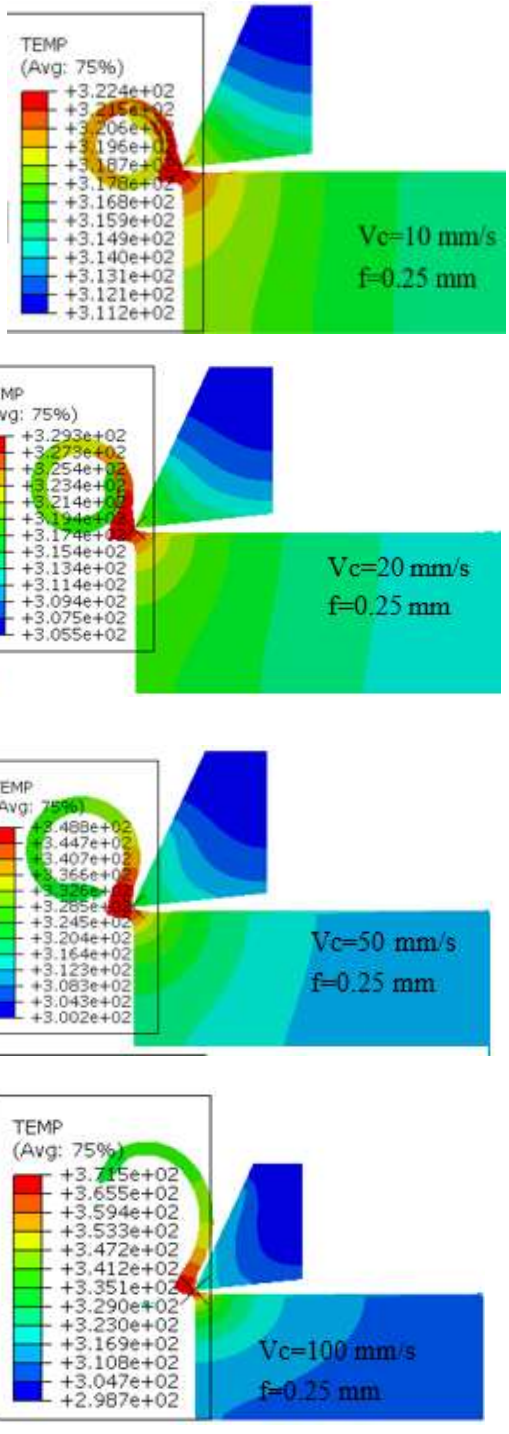

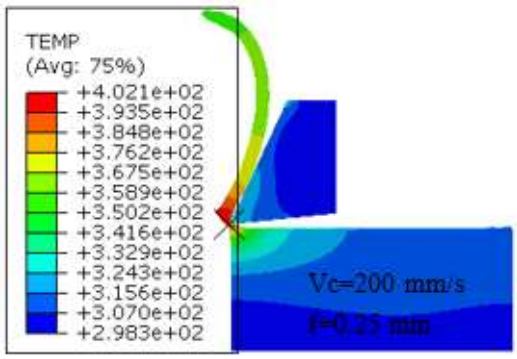

Fig. 7. Set of thermal stress behavior and chip formation of cutting metal with increasing speed

Table 5. Maximum temperature in chip formation

Impact speed [mm/s]	Depth of cut [mm]	Temperature Max., [K]
10	0.25	322
10	0.5	327
20	0.25	329
20	0.5	333
50	0.25	348
50	0.5	331
100	0.25	371
100	0.5	347
200	0.25	402
200	0.5	401

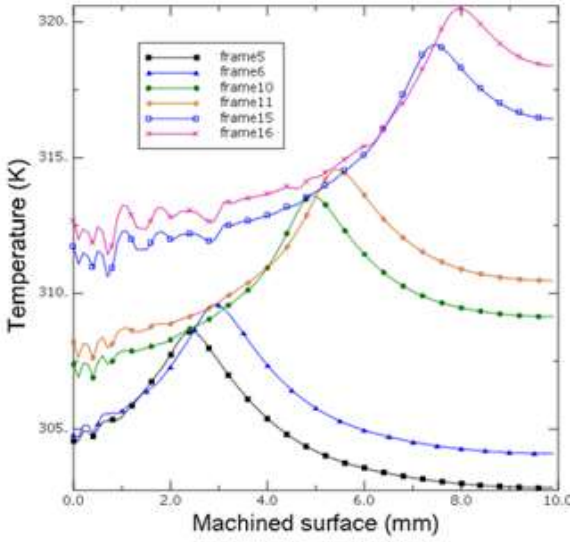

Fig. 8. Moving sources in cutting 2024-T351 aluminium alloy. Temperature distribution along machined surface for Vc=10 [mm/s]

We can see that energy generation Eg par unit volume wich is noted by $\ddot{q}$ in books (Incropera, 2011); as seen in figure 8 and can be expressed linearly and distribution temperature has parabolic form displacement which explain heat transfer by conduction with moving sources (Kim, 2011) every time due to mechanical energy (plastic and friction) converted into heat.

From figures 9, 10 and 11, cutting temperature increase with increasing depth of cut along the rake

face of the tool, temperature increase with deacresing impact speed on the machined surface.

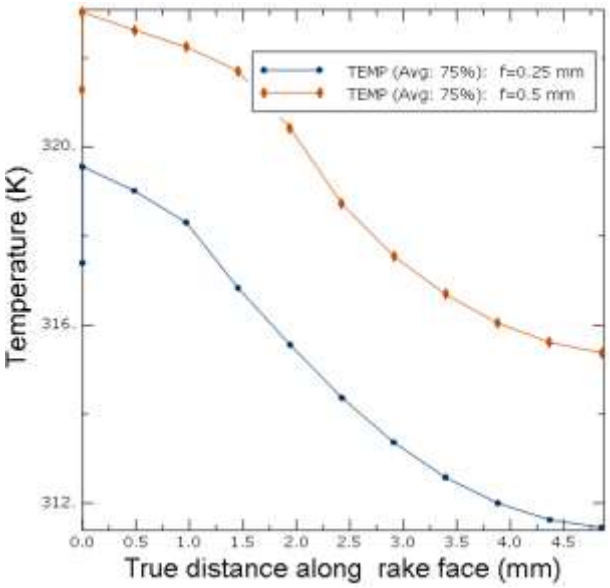

Fig.9. Temperature distribution on tool rake face

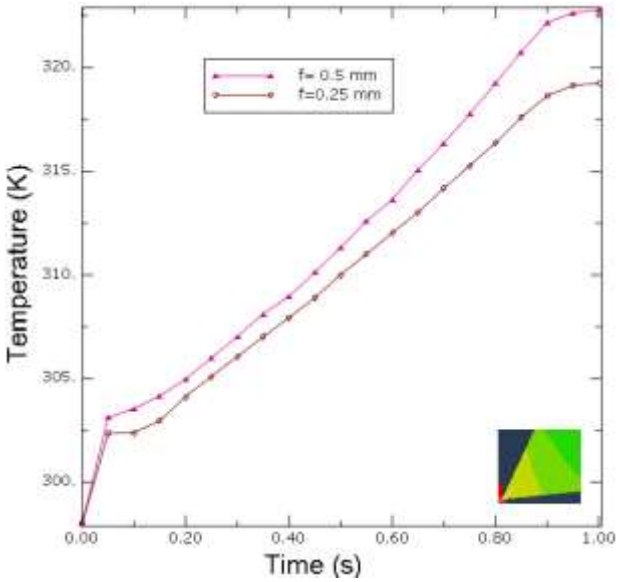

Fig. 10. Effect of depth of cut on heating of tool

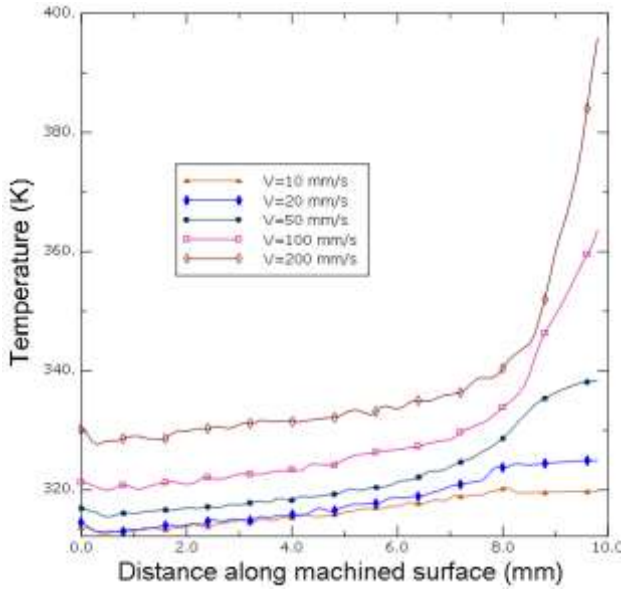

Fig. 11. Temperature distribution on machined surface

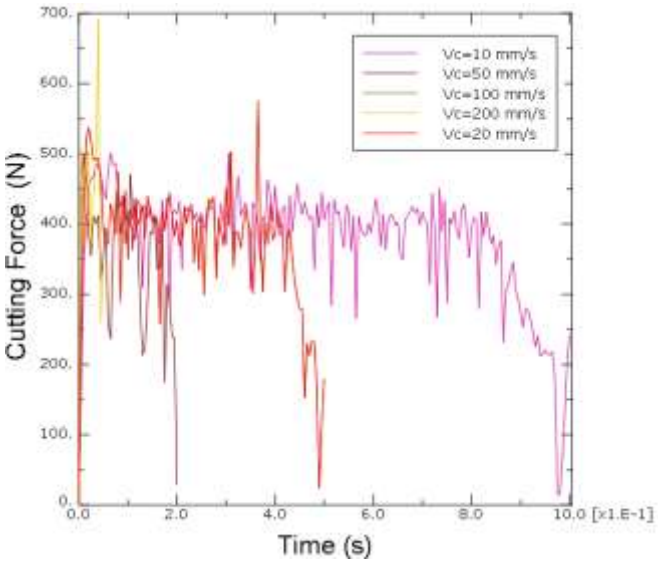

Fig. 12. Effect of increasing impact speed on cutting forces

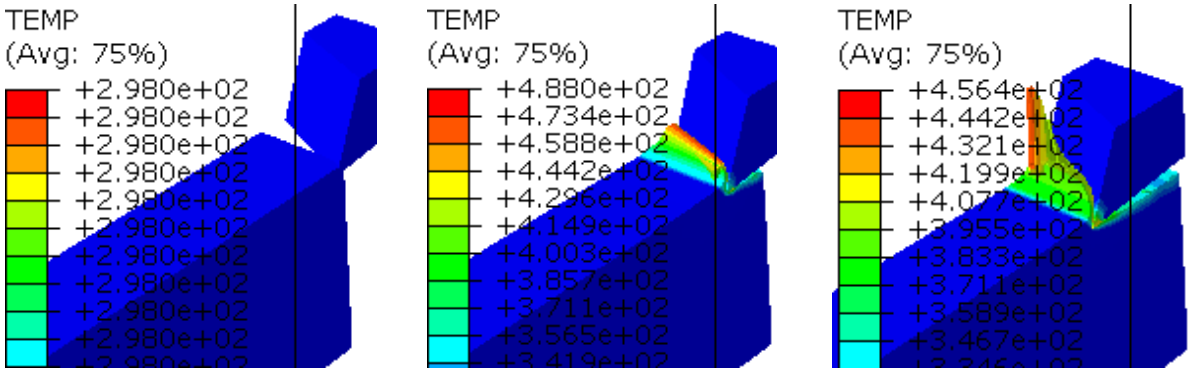

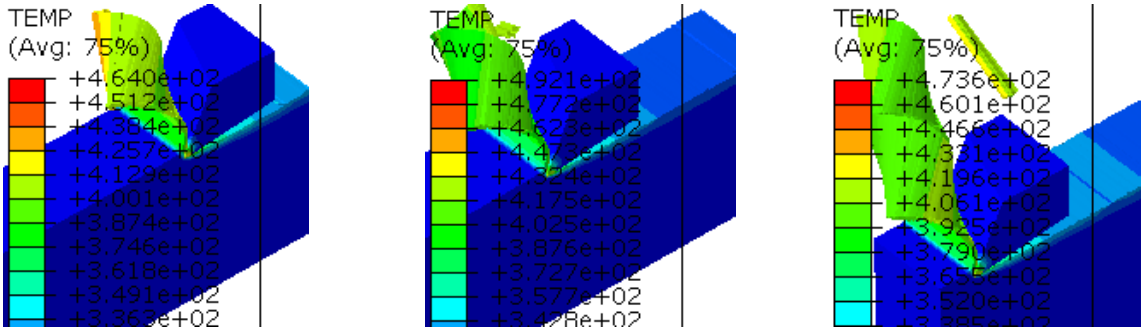

Fig. 13. Cutting temperature evolution during cutting 2024-T351 aluminium alloy in 3D

As seen in figures in three dimensions during cutting metal, the chip formation and the contact zone are very hot, however, the workpiece and the tool remain cold (adiabatic).

In summary, there are two phenomenon during cutting metal: creation, then dissipation of chip formation; when the cutting speed increase and reach the high speed machining range, the chip slide easily on the tool rake face, the specific energy decrease with decrease of total force, see figure 12 the chip became less thick, thus vibrations decrease, consequently, high surface quality is obtained. On the other hand, the contact time between chip and tool do not allow heat exchange between the chip and tool/workpiece as it was seen in conventional machining, heat dissipated with chip increase behind heat going towards tool and workpiece. Consequently, in high speed machining, dry machining is available to a large extent, [21].

3. CONCLUSIONS

In this work, a transient analysis of heat transfer during the beginning of cutting 2024-T351 aluminium simulation is performed under Abaqus dynamic explicit.

The cutting temperature is well visualized on tool workpiece assembly in 2 and 3 dimensions configurations, it has be seen that during cutting metal adiabatic assumption is imposed because heat transfer between chip formation and rake face of tool has not time to occur for increased cutting speed so We arrive to the following conclusion: energy dissipated in plastic deformation will raise the temperature of element, the heating results of *competition* between two antagonist phenomena: cutting speed and conduction between chip and tool rake face according to (Felder, 2014), [19].

Finite element method has an important role on predicting temperature value on spots which are not attainables experimentaly.

4. REFERENCES

1. Morten, F.V., (2008), *Simulation of Metal Cutting Using Smooth Particule Hydrodynamics*, 4, III(C), 17-36.

2. Huang, Y., (2003), *Modelling of the cutting temperature distribution under the tool flank wear effect*, J. of Mechanical Engineering Science, Vol. (217, Part C), 1195-1208.

3. Boothroyd, G., Eagle, J. M., Chisholm, A. W. J., (1967). *Effect of Tool and Wear on the Temperatures Generated During Metal Cutting*, Proceedings of the 8th International Machine Tool Design and Research, University of Manchester of science and technology (Manchester), 667-680.

4. Chao, B. T., Trigger, K. J., (1958), *Temperature Distribution at Tool–Chip and Tool–Work Interface in Metal Cutting*. Transactions, ASME, 1, 311– 320

5. Wiliam, Y., (2013). *Analyse de la Sensibilité et Domaine de Validité des Modélisations Analytiques de la Coupe des Métaux*, 21, *French Congres of mechanics*, Mechanics of the Metal Cutting Process, Orthogonal Cutting, (Bordeaux), 1-6.

6. Oxley, P. L. B., (1989). *Mechanics of Machining: An Analytical Approach to Assessing Machinability*, Series in mechanical engineering, pp. 6-50, *Ellis Horwood*, (Chichester).

7. Cameron Kai-Ming Chen, (2010). *Analysis of the Metal Cutting Process Using the Shear Plane Model*, Ph. D., pp.11-84, thesis, Montana State University.

8. Stevenson, M. G., Oxley, P.L.B., (1969), *An Experimental Investigation of the Influence of Speed and Scale on the Strain-rate in a Zone of Intense Plastic Deformation*, Proceedings, Institute of Mechanical Engineering, 184(1), 561-576.

9. Schermann T., Marsolek J., Schmidt C., Fleischer J., (2005). *Aspects of the Simulation of a Cutting Process with ABAQUS/Explicit Including the Interaction between the Cutting Process and the Dynamic Behavior of the Machine Tool*, 9th CIRP International Workshop on Modeling of Machining Operations, Institute of Production Science, 9, pp. 163-170, (University Karlsruhe).

10. Everton, R., (2014). *Finite Element Simulation of Chip Formation in Machining Process*, Academia Education, pp.1-11, University of Estado di Santa Catarina, DEM, Alumnus, Brasil.

11. Escamilla, I., (2010). *3D Finite Eement Simulation of the Milling Process of a TI 6 AL 4V*

Alloy, Simulia Customer conference, pp.1-10, Providence, Rhode Island, USA.
12. Umbrello, D. (2008), *Finite Element Simulation of Conventional and High Speed Machining of Ti6AL4V Alloy*, Materials Processing Technology, 196, 79-87.
13. Tuğrul Ö., Erol Z., (2005), *Finite, Element Method Simulation of Machining of AISI 1045 Steel With A Round Edge Cutting Tool*, Industrial and Systems Engineering Rutgers, pp. 533-542, USA.
14. Incropera, F.P, (2011), Fundamentals *of Heat and Mass Transfer*, John Wiley and Sons Inc., pp.142-150, California, USA.
15. Arrazola P.J., (2013). *Recent Advances in Modelling of Metal Machining Processes*, Manufacturing Technology, 62, 695-718.
16. Short, A., Bâker, M., *(*2012). *Determination of Johnson&Cook Parameters from Machining Simulations*, Computational Materials Science, 52, 298-304
17. Chattopadhyay, A. B., (2005), *Cutting Temperature Causes, Effects, Assessment and Control*, pp. 1-14 (Edition Kharagpur), India, ME IIT.
18. Kim C-K, (2011). *The Theory of Moving Sources of Heat and its Application to Metal Treatments***,** Mech. Science and Technology, 25, 895-899.
19. Felder, E., (2014), *Thermal Effect when Forming, J. of* Eng. Techn. Vol. (M 3012v2), pp. 1-24.
20. Dassault Systems, (*2013),* Abaqus Unified FEA. http://www.3ds.com/fr/produits-et-Services/simulia/produits/abaqus/, accessed 10/08/2018
21. Zaquini, L., (2003). *High Speed Machining (HSM), Origin, applications, perspectives*, article appeared in MARCHE SYSTEMES MANAGEMENT, 1, pp.1-8.
22. Tomasz, W., Yingbin B., (2005), *Calibration and evaluation of seven fracture models*, International Journal of Mechanical Sciences, 47(1), 719-743.
23. Haddag, B., Atlali, S., Nouari, M., Barlier, C. and Zenasni, M., (2012), *Analysis of the Cutting Parameters Influence During Machining Aluminium Alloy A2024-T351 with Uncoated Carbide Inserts*, Engineering Transactions, 60, 31-39.
24. Y. Ayed, (2017), *Thermo-mechanical characterization of the Ti17 titanium alloy under extreme loading conditions*, Int J. Adv. Manuf. Technol., 90, 1597-1598.

Received: August 10, 2018 / Accepted: December 15, 2018 / Paper available online: December 20, 2018